

Measurements and a model for the enhancement of Lyman- α radiation following foil-induced dissociation of molecular ions

R. L. Brooks* and H. G. Berry

Physics Division, Argonne National Laboratory, Argonne, Illinois 60439

(Received 20 July 1981)

Measurements of the enhanced Lyman- α radiation following beam-foil excitation of H_2^+ and H_3^+ molecular ions are presented for incident ion energies of 0.2–1.75 MeV/amu. The enhancement is with respect to radiation observed with the use of incident protons of the same velocity. This enhancement is small (factors of 2–10) at large foil dwell times (greater than 1 fs) and large (factors of 50) at small dwell times (less than 1 fs). A phenomenological model which fits the data for both dwell-time regions, and at the same time fits other results of the transmission of H_2^+ and of the production of H^0 atoms from incident H_2^+ ions, is presented.

I. INTRODUCTION

The interaction of fast molecular-ion beams with solid targets has received extensive scrutiny in recent years.¹ Much of the work has been performed using ion beams in the energy range of 0.2–2.0 MeV/amu which pass through thin self-supporting carbon foils. In this work we shall restrict ourselves to presenting data acquired only with hydrogen molecular-ion beams (both H_2^+ and H_3^+) and to offering comparisons to other experiments performed exclusively with H_2^+ , the simplest molecule.

It now is well established that molecular ions can survive passage through thin carbon foils.² The penetration depth of a projectile in a foil has most often been described by its dwell time, the time spent in the foil. One can then distinguish two classes of survival for molecular ions. For very short dwell times ($\lesssim 0.5$ fs), the electrons incident with the molecule maintain some correlation with the nuclei while in the target and the ion may emerge in a stable molecular state. This short dwell-time region has been labeled the \mathcal{O} regime for survival of the originals. For longer dwell times, correlation of the nuclei with the original electrons is lost and capture of target electrons close to the exit surface may occur. This has been called the \mathcal{R} or reconstituted regime.² One should not lose sight of the fact that even for the thinnest foils and highest beam velocities employed, molecular breakup with ionization of the fragments is the dominant occurrence.

The \mathcal{O} regime has also been clearly observed in an experiment in which neutral hydrogen atoms

were detected after passage through a foil upon which neutral atoms were incident.³ This experiment yielded a lifetime for neutral survival in the foil of 0.2 fs, which is taken to be characteristic of the \mathcal{O} regime.

We shall present measurements of optical emission from $n=2$ to $n=1$ (Ly α) in neutral hydrogen obtained with beams of H_2^+ and H_3^+ after passage through a thin carbon foil. Many foils with a range of nominal thicknesses from 1.5 to 92 $\mu\text{g}/\text{cm}^2$ were used. Incident beam energies from 0.2 to 1.75 MeV/amu were also used. These measurements extend and complement previous studies performed in this laboratory using incident molecular ions.^{4,5}

Comparison of the results using an incident H_2^+ beam will be made to a phenomenological model presented here for the first time. Measurements by other workers of emergent H_2^+ and H^0 with an incident H_2^+ beam under comparable beam energy and foil conditions will also be compared to the model predictions.

II. EXPERIMENTAL METHOD

Mass analyzed beams of H_2^+ and H_3^+ from the Argonne 5-MV Dynamitron were employed in a standard beam-foil configuration. Up to 20 foils at a time with differing thicknesses could be mounted on a foil wheel positioned approximately 1-mm up beam from the focusing position of the optic axis. One or two positions on the wheel contained a double foil; that is, two foil supports mounted together such that the foils were separated by about

3 mm. The radiation was monitored at right angles to the beam through a 1-m, vacuum, normal incidence, McPherson monochromator equipped with an EMR solar blind photomultiplier. Standard photon counting techniques were employed.

For a selected beam energy and mass number (2 or 3) the foil wheel was positioned to a gap and the beam current recorded. Counts were then acquired for a preset time using the double foil followed by each foil on the wheel in turn, finishing with the double foil. The current was then recorded with no foil in position. The beam was stable during the time for each measurement and corrections for slow drift in the beam current (less than 10%) were then applied to the entire set during analysis. The procedure was repeated for a selection of beam energies with data acquired using both H_2^+ and H_3^+ ions from the accelerator.

Data acquired with the double foil are interpreted as being equivalent to those of a proton beam of the appropriate current. Results presented below are intensities divided by the double foil value.

No attempt was made to remeasure the thicknesses of the foils used. Previous measurements in this laboratory indicate that the foils are nominally the thickness indicated to within 20%. Most of the scatter of our data is caused by uncertainty in the foil thickness; however, approximately 40 different foils were used for the data presented which significantly alleviates the problem caused by using the nominal thicknesses.

III. EXPERIMENTAL RESULTS

The intensity of Lyman- α emission as a function of foil thickness and beam energy will be presented in a manner that removes much of the energy dependence. The data are first normalized to the double foil values (which are strongly energy-dependent) and then graphed versus foil dwell time, t_d , given by

$$t_d = \frac{T}{v_0} \left[1 + \frac{1}{4} \left(\frac{dE}{dx} \right) \frac{T}{E_0} \right]. \quad (1)$$

Here T is the foil thickness, E_0 the incident beam energy with velocity v_0 , and (dE/dx) the energy loss per unit thickness in the foil. This is equivalent to dividing the foil thickness by the beam velocity at the center of the foil. A carbon foil density of 2.0 g cm^{-3} has been assumed.

Recently it has been suggested that data obtained

with an incident diatomic molecular ion should be graphed versus internuclear separation of the composite particles.⁶ By doing so, data taken at energies differing by a factor of 100 can be shown to lie on a smooth curve. Since neither our data nor those of others presented later for comparison differ in energy by nearly so great a factor, we have chosen dwell time for expediency. Furthermore, this permits direct comparison of the H_2^+ and H_3^+ experiments.

Figure 1 displays our results taken with an incident beam of H_2^+ while Fig. 2 is for a beam of H_3^+ . The division of the figures into two parts represents more than just an extension of the abscissa. The two are also entirely different experiments with no common data points. The procedure of double foil normalization described above holds for the shorter dwell-time data (a). Double foil values were not acquired for the longer dwell-time data (b), and each energy was normalized to minimize scatter of the composite graph. This explains the occurrence of some data points of (b) with values less than unity.

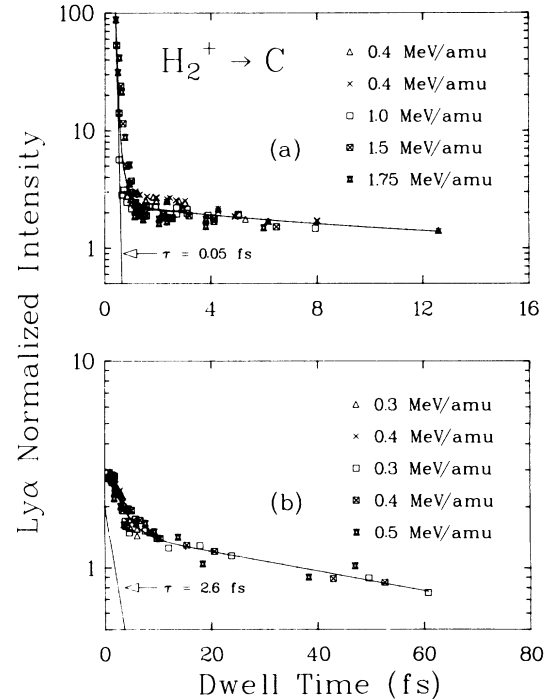


FIG. 1. Lyman- α emission as a function of dwell time in the foil for H_2^+ incident projectiles. Short and long dwell-time data are given separately and are from different experiments. The lines represent three (a) and two (b) exponential fits to the data with shortest life-times labeled.

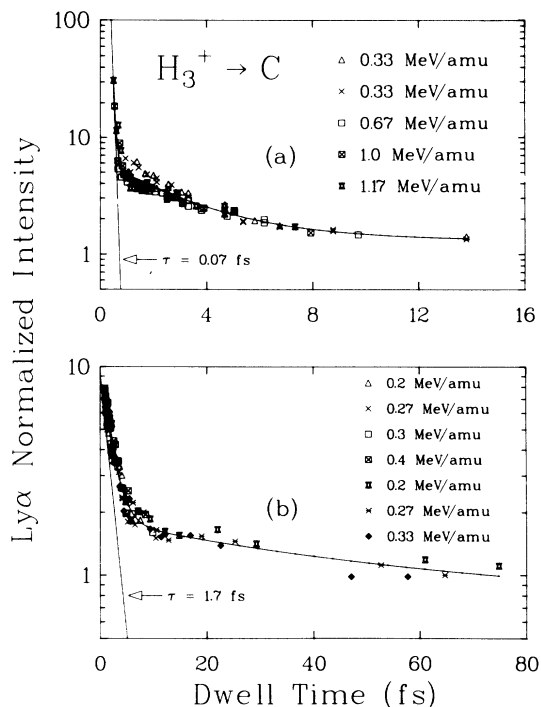


FIG. 2. Lyman- α emission as a function of dwell time in the foil for H_3^+ incident projectiles. The lines represent fits as in Fig. 1.

The smooth curves are multiexponential fits to the data with the lifetimes of the shortest components shown. The data of (a) and (b) for both figures have been independently analyzed and no common parameters appeared. Considering the significant overlap in the region of 1 to 12 fs, one is forced to conclude that no interpretation can be applied to these derived lifetimes. In particular, the shortest value quoted, 0.05 fs, has a large uncertainty; we conclude it represents some component smaller than 0.2 fs. The purpose in displaying the curves is to indicate that a multiexponential form is adequate to smoothly fit the data and this fact will help to justify the model presented below.

The curves obtained at different energies should not necessarily be the same. Small and usually consistent differences can be observed. However, these differences will be generally neglected in the analysis which follows. Further comments on this energy independence will be made later.

The enhancement of Lyman- α radiation for very short dwell times is genuinely dramatic. The sharp rise as the dwell time is reduced is clearly indicative of the \mathcal{O} regime though neutral hydrogen was not incident upon the foil. What is perhaps more

interesting is the rise visible at the beginning of the longer dwell-time curves (b). This can be interpreted as the enhancement of the probability for electron capture by the presence of a nearby proton. This interpretation is reinforced by noting that this enhancement is larger for incident H_3^+ than for incident H_2^+ . Furthermore, this longer dwell-time curve (b) is itself composed of at least two very different lifetime components which probably indicates that more than one mechanism is responsible for electron capture.

While it has been suggested⁷ that capture of an electron into repulsive molecular orbitals may be responsible for some observations in the \mathcal{R} regime, no quantitative mechanism has previously been advanced. In Sec. IV we show that the simple electron-loss and electron-capture method used by Gaillard *et al.*³ to explain the \mathcal{O} regime result with incident H^0 can be extended to simultaneously explain both the \mathcal{O} and \mathcal{R} regimes using incident H_2^+ .

IV. MODEL DESCRIPTION

Figure 3 presents a potential-energy-level diagram⁸ for H_2^+ . The inset clearly demonstrates the collapse of six molecular orbitals to three Stark shifted atomic levels. The central level is doubly degenerate composed of $2p_1$ and $2p_{-1}$. Note that even at 90 a.u. (48 Å) the energy splitting is a factor of 200 times larger than the neutral hydrogen fine structure, thereby justifying the neglect of spin.

Our model simplifies this potential-energy diagram into a system of five levels represented by Fig. 4. The molecular ion H_2^+ is on the left-hand side while the neutral atom H^0 is on the right-hand side. Level 1 represents those two molecular orbitals which in the limit of large internuclear separation become the $n = 1$ energy level of the neutral atom. Similarly, level 2 represents those six orbitals which become the $n = 2$ energy level of the neutral atom. Level 3 represents the ground state of the neutral atom, while level 4 is the first excited state. Level 5 represents the continuum, common to both the atom and molecular ion which corresponds to the beam projectiles made up entirely of protons. Pickup of two electrons leading to the neutral molecule or to the negative hydrogen ion is not considered.

The σ_{ij} represent a number of different processes. Those associated with upward pointing arrows ending in the continuum can be thought of

for $i = 1$ or 2 . The dwell time appearing in this expression should more properly be internuclear separation. If it were, there would appear a minimum separation which can be accounted for by introducing a cutoff at t_c , chosen to be 1 fs. The consequences of choosing some other value will be mentioned in the discussion below.

The exponential form for this function is motivated by the multiexponential behavior attributed to the experimental results presented above. Additionally, such exponential dependence has been observed by others in the \mathcal{R} regime for molecular-ion reconstruction.³

The solution to Eq. (2) can now be solved on a selection of logarithmically spaced intervals with t_0 representing the starting point of the interval. The initial conditions for any interval are given by the values at the last point of the previous interval. In this way, the coefficients A_j of the solution acquire some unspecified time dependence which is dominated by the functional form chosen by Eq. (8). The solution was obtained numerically for reasonable choices of σ_{ij} and α_i . The results, represented by a column of numbers for $f_1 - f_5$, were then graphed and f_1 , f_3 , and f_4 were compared to experimental measurements, after accounting for postfoil evolution of the system as described below. The process was repeated until rather good agreement for each of these three-level populations was achieved utilizing a single set of input parameters.

V. DISCUSSION OF RESULTS

Results of the model presented above will be compared to three different experiments in this section. It should be stated at the outset that these experiments are insufficient to determine all 12 model parameters. For example, the five atomic parameters on the right-hand side of Fig. 4 cannot be determined, and the chosen values have been based upon previous measurement as discussed below.

Table I lists the values of the model parameters (in fs^{-1}) used to obtain the curves presented in this section. Before comparison can be made to experimental results, postfoil evolution of the system needs to be taken into account. The populations of the levels in Fig. 4 upon exit from the foil are not the same as the populations in the detection region of a given experiment. The assumptions used to obtain values for comparison shall be given for each of the experiments concerned.

TABLE I. Model Parameters (in fs^{-1}).

Molecular Ion	Neutral Atom
$\sigma_{51} = 6.9$	$\sigma_{53} = 4.5$
$\sigma_{21} = 1.1$	$\sigma_{43} = 0.5$
$\sigma_{52} = 30$	$\sigma_{54} = 30$
$\sigma_{15}^0 = 0.0038$	$\sigma_{35} = 0.0016$
$\sigma_{25}^0 = 0.0012$	$\sigma_{45} = 0.00105$
$\alpha_1 = 0.7 \quad \alpha_2 = 0.08$	

Most of the molecular ions emerging from the foil in level 2 will continue to dissociate and will add to the population of level 4 within at least 1 ps of exit. This follows from the fact that three of the six molecular orbitals comprising level 2 are strictly repulsive while two of the remaining three have extremely shallow (< 0.3 eV) potential wells. The fraction of level 2 which does not dissociate will be accounted for below. The fraction, then, which has been added to level 4 is 0.998, or essentially the entire population. Figure 5 displays the results of the population of level 4 in the detection region along with the data presented in Fig. 1. The curve has been renormalized by setting the very long dwell-time value to unity, the same procedure as used for the data. Exactly the same curve appears in both parts of Fig. 5. Agreement

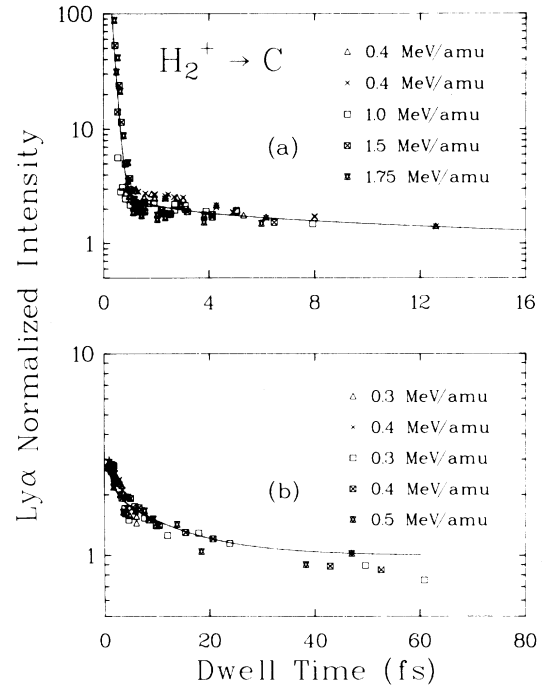


FIG. 5. Model fit to the Lyman- α emission as a function of foil dwell time (the same data as in Fig. 1).

with the data is excellent.

Level 1 is composed of two molecular orbitals; one is the ground state of H_2^+ while the other is strictly repulsive and dissociates into level 3. A dissociation fraction of 0.75 has been chosen as this yields somewhat better agreement with the experimental results than the purely statistical choice of 0.5. Figure 6 displays the results for level 1 in the detection region and compares it to the data given in Cue *et al.*² Normalization has been accomplished by dividing the population of level 1 in the detection region by the predicted model value of the neutral fraction of H^0 for a very long dwell time. This is the model analog of the manner in which the data were normalized. Better agreement with the data beyond about 12 fs can be obtained by adding to level 1 0.2% of the population of level 2. This small admixture from level 2 represents either radiation from the $2p\pi_u$ or survival of the H_2^+ ion in the excited state. While the $3d\sigma_g$ orbital contains the largest potential well of level 2, electric dipole transitions from that orbital terminate on the $2p\sigma_u$ which is strictly repulsive and such transitions cannot increase the population of bound H_2^+ ions. The population in this $3d\sigma_g$ orbital has been improperly added to the population of level 4. This is of no consequence, however, since the adjustment of an indeterminate model parameter (σ_{52}) could compensate for the effect upon level 4. This seemed preferable to introducing an additional "branching ratio" which would, with present experiments, be indeterminate. Should radiation from the H_2^+ molecular ion be detected, the results could readily be accommodated by this model and would significantly reduce the indeterminacy of the parameters described below.

The third experiment to which we compare this model was performed by Gaillard *et al.*³ who measured the neutral fraction of H^0 using a beam of H_2^+ . This total neutral fraction is then the population of level 3, along with 75% of level 1, and the entire population of level 4 when it passed through its detection zone. Figure 7 compares this result with the aforementioned data. Renormalization has been accomplished by setting a very long dwell-time value to unity.

The postfoil evolution for each of the three experiments can be summarized as

$$H^0(n=2) = (f_4 + af_2)/N_1, \quad (9)$$

$$H_2^+ = [(1-b)f_1 + (1-a)f_2]/N_2, \quad (10)$$

$$H^0 = (f_3 + bf_1 + f_4 + af_2)/N_2, \quad (11)$$

where $a=0.998$ and $b=0.75$. The normalization

factors N_1 and N_2 are given by

$$N_1 = f_4(t = \infty), \quad (12)$$

$$N_2 = f_3(t = \infty) + f_4(t = \infty). \quad (13)$$

Before examining which model parameters in Table I influence dominant features in Figs. 5–7, it will prove useful to examine the \mathcal{O} regime in detail. Figure 8 presents the relative level populations upon emerging from the foil for dwell times less than 1 fs. The first notable feature is that 99% of the incoming beam is stripped of its electron in less than 0.6 fs. The straight-line portion of f_1 has a lifetime of $1/(\sigma_{21} + \sigma_{51})$ or 0.12 fs. That f_2 appears to have the same lifetime is a consequence of the large value of σ_{52} and the fact that the population is initially fed into this level through level 1. Postfoil evolution will then attribute this short lifetime value to both the H^0 ($n=1$) and H^0 ($n=2$) levels and this contributes to the sharp rise in the curves of Figs. 5 and 7 below 1 fs. This lifetime is then characteristic of the \mathcal{O} regime for incident H_2^+ molecules. The value is somewhat less than 0.2 fs which was determined by Gaillard *et al.*³ for

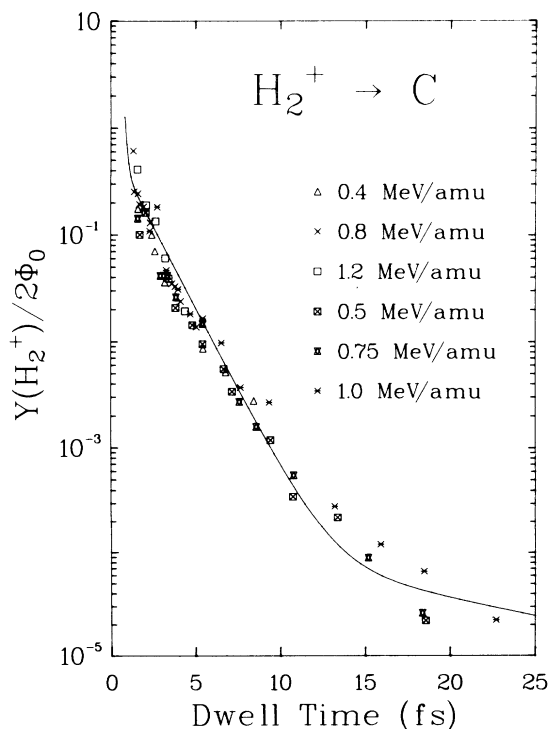


FIG. 6. Model fit to transmission probability of H_2^+ through thin carbon foils, normalized to twice the atomic neutral fraction, as a function of the foil dwell time. Data from Ref. 2.

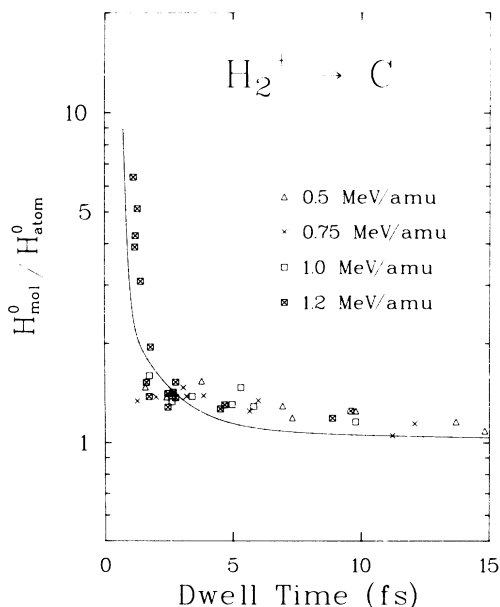


FIG. 7. Model fit to the production probability of neutral hydrogen molecules, normalized to the atomic neutral fraction, as a function of the foil dwell time. Data from Ref. 3.

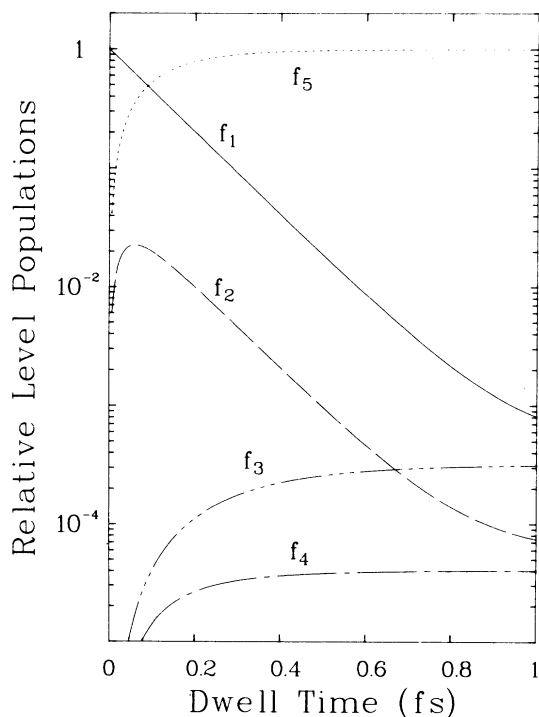


FIG. 8. The relative level populations $f_1 - f_5$ at the foil exit surface, for the rate constant values given in Table I, as functions of the foil dwell time.

incident H^0 . It is also greater than the curve-fitting value of 0.05 fs (Fig. 1) but, as mentioned previously, that number has a large uncertainty. According to this model, the value of 0.2 fs measured for incident H^0 particles should be attributed to $1/(\sigma_{43} + \sigma_{53})$, and indeed this number has been used to establish that sum.

The curves marked f_3 and f_4 in Fig. 8 show that electron-capture and electron-loss equilibrium is established in about 0.4 fs, which means that capture of an electron must occur close to the final surface for the electron to emerge bound to the projectile. This is the way an intrinsically “bulk” model points out the importance of surface and near surface interactions in the \mathcal{R} regime.

Three experiments have been satisfactorily described by a model containing 12 parameters (10 σ_{ij} ; $2\alpha_i$). Additionally, there appeared the cutoff t_c and two postfoil branching ratios a and b . The method used to determine these latter two has already been described. Any value for t_c less than 1 fs could be accommodated by simply increasing, σ_{i5}^0 ($i = 1, 2$). Values much larger than 1 fs would first manifest themselves by producing an observable “dimple” on the curve of Fig. 6 close to t_c , which, as t_c became greater, would become an unacceptably large discontinuity in the slope of the curves of Figs. 5–7.

Results in the \mathcal{R} regime are influenced most by the molecular capture rate constants σ_{15} and σ_{25} which are functions of α_1 and α_2 . $1/\alpha_1$ is an effective lifetime which determines the slope of the curve in the straight-line portion of Fig. 6. $1/\alpha_2$ controls the decrease in the curves of Fig. 5 beyond about 4 fs. Within the framework of this model, both of these parameters are well determined.

The question of nonuniqueness for the ten σ_{ij} parameters can best be examined by considering the five molecular or atomic rate constants separately. Among the molecular rate constants, four relations are well determined: $\sigma_{51} + \sigma_{21}$, $\sigma_{15}^0 / (\sigma_{51} + \sigma_{21})$, $\sigma_{21} / \sigma_{52}$, $\sigma_{25}^0 / \sigma_{52}$. σ_{52} has been arbitrarily set to a “reasonable” value which satisfies the constraint $\sigma_{52} > (\sigma_{51} + \sigma_{21})$.

The five analogous atomic parameters cannot be determined from the experiments presented here. However, comparison to the experiment by Gailard *et al.*³ using an incident H^0 beam allows $(\sigma_{43} + \sigma_{53})$ and σ_{35} to be determined, assuming a beam energy of 1.2 MeV/amu. (Energy dependence will be considered below.) The excitation rate constant σ_{43} has been chosen by appeal to the theoretical work of Peterkop and Veldre.⁹ The ra-

tio σ_{45}/σ_{54} has been chosen such that the equilibrium population of H^0 ($n=2$) is $\frac{1}{8}$ that of H^0 ($n=1$). σ_{54} has been set equal to σ_{52} .

Figures 5–7 present the experiments and the model results in such a way as to remove much of the energy dependence in the parameters from consideration. By normalizing the model results to the very long dwell-time equilibrium values of f_3 and f_4 , one has effectively eliminated the energy dependence of σ_{45} and σ_{35} . Implicit in the model is the assumption that the other σ_{ij} parameters are energy independent. Over the rather narrow energy range of these experiments that assumption may be justified. There is no reason, from the model viewpoint, why energy dependence could not be imposed. For the present, however, it appears that the experiments are not sufficiently refined to warrant separate analysis for each measured energy.

VI. CONCLUSIONS

We have presented measurements of Lyman- α intensity following molecular-ion dissociation in thin carbon foils. Using both H_2^+ and H_3^+ projectiles, an enhancement in this intensity of more than 50 over that using atomic projectiles has been observed for very thin foils at high velocity. By attributing this enhancement to dissociation of electronically excited states of the molecular ion, a conceptually simple, phenomenological model has

been motivated. Using a single set of model parameters, the results of three experiments have been satisfactorily reproduced by this model.

Whether such model parameters can prove to be quantitatively useful will depend upon further theoretical work on electron capture into excited-state molecular orbitals. The model of Cue *et al.*² seems to indicate that multiple-scattering effects are responsible for what appears in our model as the exponential decay of the molecular-ion electron-capture rate constants. The complexity of their model, especially if applied to the next six molecular-ion orbitals, precludes any simple correspondence with our capture rate constants. Only further work may help us to decide whether our qualitative approach can be sufficiently refined to yield meaningful capture and loss cross sections for molecular ions.

ACKNOWLEDGMENTS

We wish to thank Jonathan Hardis for his help with data collection and Jim Ray for technical assistance during these experiments. Special thanks are extended to B. J. Edwards for suggestions regarding notation and to Don Gemmell for helpful discussions. This research was supported by the U. S. Department of Energy, Office of Basic Energy Sciences, under Contract No. W-31-109-Eng-38.

*Present address: Department of Physics, University of Guelph, Guelph, Ontario N1G 2W1.

¹See, e.g., *Atomic Collisions in Solids*, edited by D. P. Jackson, J. E. Robinson, and D. A. Thompson, in *Nucl. Instrum. and Methods* **170**, Part II (1980).

²N. Cue, N. V. de Castro-Faria, M. J. Gaillard, J. C. Poizat, J. Remillieux, D. S. Gemmell, and I. Plessner, *Phys. Rev. Lett.* **45**, 613 (1980).

³M. J. Gaillard, J. C. Poizat, A. Ratkowski, J. Remillieux, and M. Auzas, *Phys. Rev. A* **16**, 2323 (1977).

⁴Gerald Gabrielse, *Phys. Rev. A* **23**, 775 (1981).

⁵T. J. Gay, H. G. Berry, and R. DeSerio, *Phys. Rev. A*

23, 1761 (1981).

⁶Timothy R. Fox, *Nucl. Instrum. and Methods* **179**, 407 (1981); W. H. Escovitz, T. R. Fox, and R. Levi-Setti, *IEEE Trans. Nucl. Sci.* **NS-26**, 1395 (1979).

⁷J. Remillieux, Ref. 1, p. 31.

⁸Marcella M. Madsen and James M. Peek, *At. Data* **2**, 171 (1971).

⁹R. Peterkop and V. Veldre, in *Advances in Atomic and Molecular Physics*, edited by D. R. Bates and Immanuel Estermann (Academic, New York, 1966), Vol. **2**, p. 263.